

CFD Simulation of Gaseous Suppressant Injection and Fire Extinguishing

D. MAKAROV* and A. KARPOV

All-Russian Research Institute for Fire Protection
VNIPO-12, Balashiha-3, Moscow region, 143900 Russia

T. TSURUDA

National Research Institute of Fire and Disaster (Japan)
14-1, Nakahara 3-chome, Mitaka, Tokyo 181, Japan

ABSTRACT

This paper describes the comparison of the theoretical solution and the CFD modelling of isothermal suppressant mixing and gaseous fire suppression. Two different types of boundary conditions, applied for the suppressant distribution modelling, were tested. The cost-effective problem formulation was used for the modelling of the real fire extinguishing experiment. Three suppressant injection methods were applied for the same compartment geometry and fire scenario during the numerical simulation. All injection methods produced almost the same amount of suppressant in compartment during the numerical simulation, but different suppressant distribution and different time and effectiveness of the fire extinguishing. It is shown that the refined analysis of extinguishing system performance must be based on the detailed information about suppressant distribution and heat release rate behaviour. The use of CFD technique for this purpose is very effective.

KEYWORDS: CFD, model, theoretical solution, boundary conditions, extinguishing.

NOMENCLATURE

c_p	Specific heat for constant pressure (J/kg/K)
$c_\mu, c_1, c_2, \sigma_k, \sigma_\epsilon$	Standard k - ϵ turbulent model constants
g_i	Acceleration along x_i axis (m/s ²)
h	Enthalpy (J/kg)
k	Turbulent kinetic energy (m ² /s ²)
M	Mass (kg)
\dot{M}	Mass injection rate (kg/s)
p	Pressure (Pa)
R	Gas constant (J/kg/K)
S	Source term in conservation equation
Sc_t	Turbulent Schmidt number (--)
s	Stoichiometric ratio (--)
T	Temperature (K)
\vec{u}	Velocity vector (m/s)
u_i, u_j, u_k	Velocity components (m/s)
V	Volume (m ³)

* Author for correspondence

\dot{V}	Volume injection rate (m ³ /s)
v	Volume concentration (—)
Y	Mass concentration (—)
Y_{spr}^*	Flame extinguishing concentration of suppressant (—)
x_i, x_j, x_k	Spatial coordinates (m)
χ	Energy fraction, lost due to radiation (—)
ϵ	Dissipation rate of turbulent kinetic energy (m ² /s ³)
Φ	Common scalar variable
μ_t	Turbulent viscosity (Pa·s)
ρ	Density (kg/m ³)
σ_t	Turbulent Prandtl number (—)
τ	Time (s)

Subscript

<i>amb</i>	ambient
<i>u</i>	uniform
<i>cmp</i>	compartment
<i>spr</i>	suppressant
<i>fl</i>	fuel
<i>ox</i>	oxygen
<i>inflow</i>	at inflow of calculation domain
<i>outflow</i>	at outflow from calculation domain

INTRODUCTION

The increase of fire-safety requirements and the orientation to performance based fire regulation, which is a world-wide trend now, need reliable engineering methods for prediction of fire dynamics and fire protection design. Fire modelling became to be a necessary tool of fire safety analysis. The development of computer technology and the progress in numerical methods made Computational Fluid Dynamics (CFD) one of the practical methods for fire modelling and the most detailed technique in the field of fire research.

In past years a lot of efforts were aimed to the problem of fire suppression modelling with use of CFD. For the most part, the influence of water spray and water mist on fire behaviour, altogether with their extinguishing mechanisms, were studied numerically. For instance, in [1-4] different extinguishing models, which describe fire suppression with water spray or water mist, were reported. The detailed literature review on modelling of two-phase flows with water drops is presented in [5]. Much less attention was paid for other fire suppressants and fire extinguishing methods. The fire suppression model for solid phase fine aerosol was described in [6] and was used also in [7]. This model prescribes the extinguishing, using the flame extinguishing concentration of suppressant.

The gaseous fire extinguishing is one of the widely used methods of fire suppression. The extinguishing mechanism for gaseous fire suppression is well studied both experimentally and theoretically. Traditionally, the simplified theoretical model is used to estimate the suppressant concentration in compartment. This model assumes the isothermal and perfect mixing of suppressant, which is far from the real injection conditions and the real temperature distribution in the case of fire.

The gaseous fire suppression is well suited for CFD modelling: it is one-phase flow, it doesn't need special models or assumptions for calculation of suppressant dynamics and its modelling must be cheap in terms of computer resources. The application of CFD methods in this field can deliver the detailed solution - suppressant concentration distribution with time, dependence on velocity and temperature fields, behaviour of Heat Release Rate (HRR) - which are hardly possible to receive using analytical or empirical models. These facts make CFD technique very attractive and valuable for study of gaseous extinguishing: analysis of suppressant distribution, evaluation of extinguishing system effectiveness, investigation of fire suppression.

EXPERIMENTAL CONDITIONS

Often, modern underground parking areas and many-stored garage compartments have complicate geometry and different technical devices, besides cars. It is very convenient to protect them from a fire, using gaseous extinguishing systems.

In this research, the compartment geometry and the fire scenario of a real fire extinguishing experiment were used for the fire suppression modelling. The experiment with a gaseous fire suppression in a three-store garage compartment was performed by Science University of Tokyo with the aim to evaluate the effectiveness of gaseous suppression system under conditions of fire in a garage.

The garage compartment is shown on Figure 1. It had sizes 5.4x6.6x5.5 m (width, length and height correspondingly). Special construction, where cars can be stored one above another, was installed inside of garage and two real cars were situated on its low and middle levels. Besides usual openings - door and window - the garage had a check valve at the floor level. The check valve allowed only gas outflow from the compartment to prevent compartment destruction due to a pressure rise during the suppressant injection.

The kerosene pool fire was set under the lower car as a fire source at the beginning of experiment, $\tau=0$ s. The second fire source was put into the car salon at the moment $\tau=480$ s. At this time, all openings were shut and the fire continued further in the closed garage until the moment $\tau=520$ s. Here, the only place, available for gas output, was the check valve. In the moment $\tau=520$ s, the fire suppression system was initiated and the gaseous suppressant was injected during 104 s with the average mass flow rate 1.23 kg/s (until the time $\tau=624$ s). The gaseous suppressant IG541 was used in this experiment. The chemical composition of IG541 is (volume fraction): N₂ 52%, Ar 40%, CO₂ 8% [8]. The suppressant injection nozzle was constructed to distribute the gas agent in the radial direction along the walls and ceiling.

During the experiment, the temperature values were obtained from 18 thermocouples, installed around cars. Also, three gas probes, for measuring CO₂ and O₂ concentrations, were set along the vertical direction near the centre of compartment.

ANALYTICAL MODEL FOR SUPPRESSANT CONCENTRATION

The suppressant concentration in a compartment can be calculated using the simple analytical method, which assumes: a) the instantaneous and perfect mixing of suppressant, while it is being injected into compartment, b) the equal volumes of injected suppressant and outgoing from a compartment gas mixture. It allows to receive the balance equation for a volume of suppressant in a compartment:

$$dV_{spr} = \dot{V}_{spr} \cdot (1 - v_{u,spr}) \cdot d\tau. \quad (1)$$

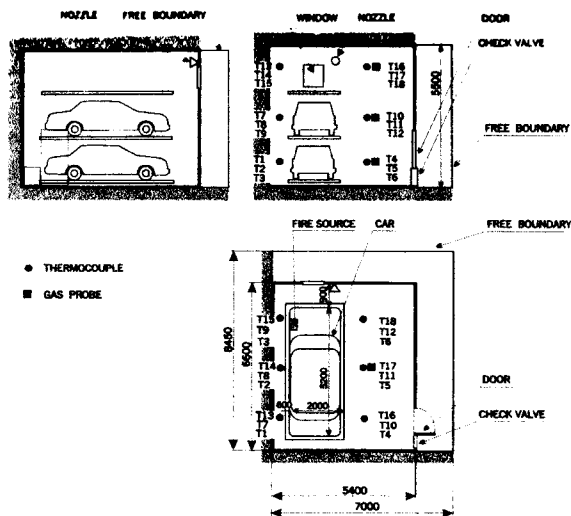


FIGURE 1. Scheme of experimental compartment and calculation domain

Being written in the term of compartment volume and integrated over the time of injection, it gives the final concentration of a suppressant in compartment:

$$v_{u,spr} = 1 - \exp(-V_{spr}/V_{cmp}) \quad (2)$$

This method of evaluation of suppressant concentration is well known and its description can be found, for instance, in [9] or [10].

The assumptions of this method mean that the suppressant concentration field in compartment is presumed to be uniform during the whole injection time – from the initial period until the final stage, and the temperature inside of compartment is constant and uniform also. Both assumptions are not correct for a real injection system and for a real fire conditions. In the case of non-uniform temperature distribution, the volume of gas, which went from a compartment, is not equal to the volume of injected suppressant. Actually, the gas flow rate at the exit from a compartment is prescribed by a pressure difference between a compartment and an ambient atmosphere, but this problem needs the use of a more sophisticated calculation methods.

The conditions of equal mass at outflow and mass of injected suppressant (mass at inflow) can be applied for the same problem easily. These boundary conditions are very useful and popular for CFD modelling of internal flows with forced convection. The conditions with equal mass rates at inflow and at outflow give the new mass balance formula:

$$dM_{spr} = \dot{M}_{spr} \cdot (1 - Y_{u,spr}) \cdot dt, \quad (3)$$

which leads to solution, similar to (2):

$$Y_{u,spr} = 1 - \exp(-M_{spr}/M_{cmp}) \quad (4)$$

The characteristics of suppressant injection during the considered experiment were molar weight of IG541 34 kg/kmol, total mass of discharged suppressant 128.5 kg, time of injection $\Delta\tau = 104$ s. At this stage, we assumed that the volume of compartment was $V_{cmp} = 174.7 \text{ m}^3$. The Figure 2 shows the results for both methods of suppressant concentration calculation for temperatures $T=293\text{K}$, $T=373\text{K}$, $T=473\text{K}$ in term of suppressant mass as a function of injection time. Total mass of the suppressant is shown also, so we can estimate the amount of suppressant, which left a compartment.

It is seen that the difference between the model (2) and the model (4) is low, about 3.5% of the total mass of injected suppressant. This difference depends on the molar weight and the amount of discharged suppressant. The assumption of equal mass rates at inflow and outflow can be used for the modelling of the suppressant propagation, if the average temperature in compartment doesn't differ too much during a suppressant injection or the suppressant is not too heavy (like CO_2 , for example). Otherwise, it will lead to a drastic discrepancy with reality.

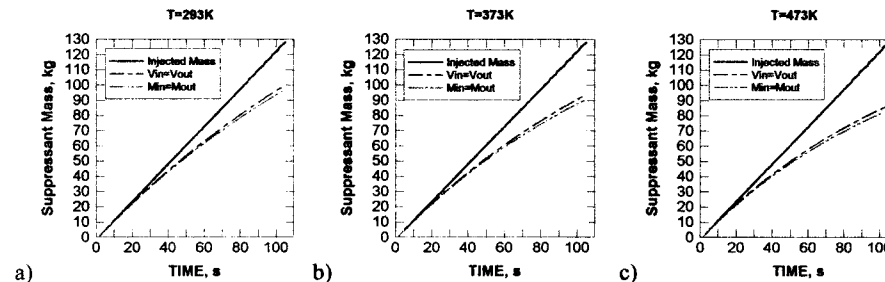


FIGURE 2. The mass of the suppressant in compartment. The theoretical solutions for perfect and isothermal mixing and different boundary conditions: a) $T=293\text{K}$, b) $T=373\text{K}$, c) $T=473\text{K}$

CFD MODELLING OF ISOTHERMAL SUPPRESSANT INJECTION

Mathematical model

In the first part of this research, the isothermal suppressant injection into garage was modelled with the aim to compare numerical results with the analytical model.

Three dimensional CFD program, used in this research, realised the control-volume based finite difference method, staggered grid for velocities and scalar variables, power-law scheme and SIMPLE algorithm for pressure-velocity coupling [11]. The mathematical model, used at this stage, consisted of following equations:

- continuity equation and momentum conservation equations

$$\frac{\partial \rho}{\partial \tau} + \frac{\partial \rho u_j}{\partial x_j} = 0, \quad (5)$$

$$\frac{\partial \rho u_i}{\partial \tau} + \frac{\partial \rho u_j u_i}{\partial x_j} = -\frac{\partial p}{\partial x_i} + \frac{\partial}{\partial x_j} \left(\mu_t \frac{\partial u_i}{\partial x_j} \right) + \frac{\partial}{\partial x_j} \left(\mu_t \frac{\partial u_j}{\partial x_i} \right) - (\rho - \rho_0) g_i, \quad (6)$$

- equations for $k-\epsilon$ turbulence model of Launder-Spalding [12] with buoyancy corrections [13]

$$\frac{\partial \rho k}{\partial \tau} + \frac{\partial \rho u_j k}{\partial x_j} = \frac{\partial}{\partial x_j} \left(\left(\frac{\mu_t}{\sigma_k} \right) \frac{\partial k}{\partial x_j} \right) + G_K + G_B - \rho \epsilon, \quad (7)$$

$$\frac{\partial \rho \epsilon}{\partial \tau} + \frac{\partial \rho u_j \epsilon}{\partial x_j} = \frac{\partial}{\partial x_j} \left(\left(\frac{\mu_t}{\sigma_\epsilon} \right) \frac{\partial \epsilon}{\partial x_j} \right) + \frac{\epsilon}{k} [C_1(G_K + G_B)] - C_2 \rho \frac{\epsilon^2}{k}, \quad (8)$$

where $\mu_t = c_\mu \rho \frac{k^2}{\epsilon}$, $G_K = \mu_t \left(\frac{\partial u_i}{\partial x_j} + \frac{\partial u_j}{\partial x_i} \right) \frac{\partial u_i}{\partial x_j}$, $G_B = -\beta g_i \frac{\mu_t}{\sigma_t} \frac{\partial T}{\partial x_i}$, $\beta = -\frac{1}{\rho} \left(\frac{\partial \rho}{\partial T} \right)_p$,

- equation for suppressant concentration

$$\frac{\partial \rho Y_{spr}}{\partial \tau} + \frac{\partial \rho u_j Y_{spr}}{\partial x_j} = \frac{\partial}{\partial x_j} \left(\left(\frac{\mu_t}{Sc_t} \right) \frac{\partial Y_{spr}}{\partial x_j} \right). \quad (9)$$

The set of equations was closed with the state equation of ideal gas $p = \rho RT$. Here, the gas mixture, consisted of two species – air and suppressant, was considered. All equations were solved in dimensional form.

Initial and Boundary Conditions

Suppressant modelling was performed for two types of boundary conditions. Forced convection type of flow in garage during suppressant injection and the only outlet opening – check valve – gives the possibility to use the boundary conditions with constant mass rate at outflow, which is equal to the suppressant mass injection rate. This type of boundary conditions is widely used for modelling of incompressible internal flows. Assumption about equal mass rates at inflow and at outflow is not correct in our case of transient solution and variable density, but it allowed to use the smaller calculation domain and the numerical grid with a low number of grid nodes. The convergence velocity and solution stability for problems with this type of boundary conditions is high enough also. In this case, the calculation domain included only garage compartment, its sizes were 5.4x6.6x5.5 m. The total number of numerical grid nodes was 44,022. Boundary conditions for this case were: constant velocity for suppressant injection at inflow, $\bar{u} = Const$, and velocity, prescribed from mass balance in compartment as it was described above, at outlet; at the walls a no-slip boundary condition was used, $\bar{u} = 0$; outflow boundary conditions were used for all scalar variables at the opening, $\partial \Phi / \partial n = 0$; suppressant concentration at inflow was $Y_{spr} = 1$. At initial moment, all velocities and suppressant concentration inside of compartment were equal to zero: $\bar{u} = 0$, $Y_{spr} = 0$; turbulence characteristics were set to low, near-zero values.

In the second model, the calculation domain included an external region, attached to the compartment with the constant pressure conditions at the boundary. Calculation domain sizes were 7.0x8.45x5.5 m in this case (see Figure 1). The boundary conditions were realised here similar to [14]: condition $p = 0$ was used at free boundaries, normal velocities were obtained from the condition $\partial u / \partial n = 0$; condition $Y_{spr} = 0$ was used for the suppressant at inflow part of free boundary and $\partial Y_{spr} / \partial n = 0$ at outflow part; the turbulence characteristics were calculated

from assumption of 5% turbulence level and ambient turbulence viscosity $\mu_t = 10^{-4} \text{ Pa} \cdot \text{s}$ at inflow of free boundary and conditions $\partial k / \partial n = 0$, $\partial \epsilon / \partial n = 0$ were set at outflow. The other boundary and initial conditions were the same as they were described for the previous case.

This second model is more realistic because the flow at compartment's outlet is received from calculation, while in the previous case it is prescribed as a boundary condition. From another side – the numerical grid for this type of calculation domain consists of bigger number of grid nodes, which makes the convergence longer and the calculation – more expensive.

The numerical grid inside of garage was the same for the both types of models: it was non-uniform grid with the characteristic size of control volume about 0.1 m near the walls and up to 0.4 m for blocked areas in obstacles. The internal volume of garage, which was free of obstacles, was 174.7 m³. During test calculations, several values of time step $\Delta \tau$ were checked: 1.0 s, 0.5 s, 0.2 s; the time step $\Delta \tau = 0.5$ s was adopted for a modelling of suppressant injection.

Three different methods of suppressant injection were modelled in this research with both types of boundary conditions. The first method of injection is the same as it was in experiment (radial spreading flow). In the second case, the suppressant was injected through one nozzle, which provided the suppressant initial velocity 55.7 m/s. In the third case, the injection through three similar nozzles was modelled, where the suppressant initial velocity was 18.7 m/s. In the second and third cases the nozzles were situated in the same vertical plane as it was in experiment (first injection method), but on the opposite wall. It was made to prevent the extremely high suppressant leakage, which could acquire if the stream spread straight to the outlet direction. The amount of suppressant and the time of injection were the same for all three cases.

Results of Simulation

Three methods of injection gained different strategies. The radial spreading suppressant flow, used in the first case, formed a wide mixing area along the walls and ceiling. In the second case, we can expect the intensive forced convection mixing due to a high speed of nozzle flow. The third case of injection was aimed to a quick filling with agent of central part of the compartment.

The Figure 3 shows the distribution of suppressant volume concentration for all three injection cases after 30 s of injection (equal inflow-outflow mass rate boundary conditions). It is possible to see that in the first case of injection the suppressant spreads along the ceiling and wall as it was designed and air in the central part of calculation domain is relatively bad mixed with the suppressant. In the second case, the suppressant is mixed much more uniformly in the centre of compartment and here its concentration is higher. For the third case, the suppressant concentration in the plane of nozzle position is less uniform than in the second case.

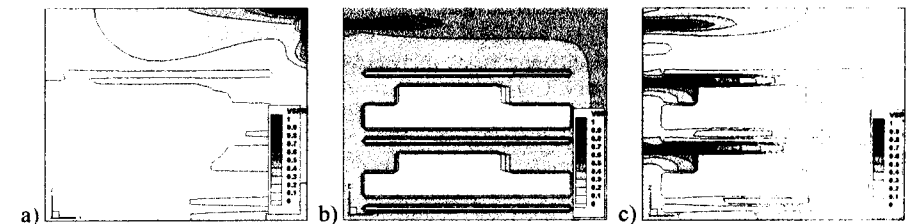


FIGURE 3. Distribution of suppressant volume concentration for injection time $\tau = 30$ s: a) radial spreading flow, b) one nozzle flow, c) three nozzle flow

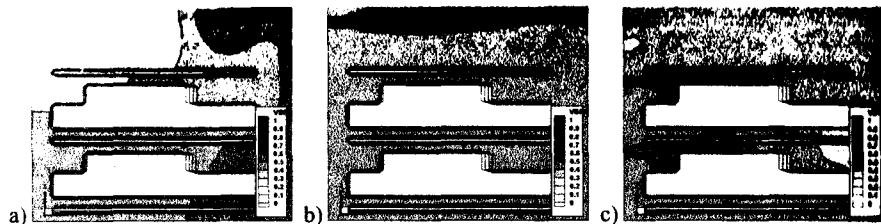


FIGURE 4. Distribution of suppressant volume concentration for injection time $\tau = 104$ s: a) radial spreading flow, b) one nozzle flow, c) three nozzle flow

Details of suppressant distribution after complete discharged of the suppressant, $\tau = 104$ s, are shown in Figure 4. At the final stage of injection, all three injection methods demonstrate more uniform suppressant mixture, but still different fields of the suppressant distribution.

The results for mass of suppressant in the compartment are presented in Table 1 for both types of boundary conditions in comparison with theoretical solution. Here, we can conclude that the numerical results for mass of suppressant in compartment generally follows results for perfect mixing, though the distribution of suppressant is not perfect. The CFD results correspond to the theoretical solution with error level up to 2.4% of total suppressant mass for the free boundary conditions and up to 1.5% for the fixed mass flow rate. It means that the mass of suppressant is relatively insensitive to the details of suppressant distribution and depends, mainly, on the mass of the discharged suppressant and the volume of compartment.

TABLE 1. Mass of the suppressant, left in compartment, for isothermal injection: results for different solutions and boundary conditions, kg

	Equal volume rates, $\dot{V}_{inflow} = \dot{V}_{outflow}$	Equal mass rates, $\dot{M}_{inflow} = \dot{M}_{outflow}$
Theoretical solution	100.20	96.20 kg
	Free boundary condition, $p=0$	Equal mass rates, $\dot{M}_{inflow} = \dot{M}_{outflow}$
Radial spreading flow	97.1	96.4
One nozzle flow	101.3	97.2
Three nozzle flow	101.3	98.2

Comparing numerical results for different types of boundary conditions, we can say that for every injection case their disagreement with each other is under the limit 3.5 % for the modelled conditions. So, for the initial stage of fire and the initial low-temperature conditions it is possible to use the less CPU-expensive calculation domain with the equal inflow-outflow mass rate boundary conditions, keeping this disagreement in the mind.

CFD MODELLING OF FIRE AND GASEOUS FIRE SUPPRESSION

Mathematical Model

The fire modelling and the modelling of the gaseous fire suppression was performed at the second stage of present research. The mathematical model (5)-(9) was added with the following equations:

- energy conservation equation

$$\frac{\partial \rho h}{\partial \tau} + \frac{\partial \rho u_j h}{\partial x_j} = \frac{\partial}{\partial x_j} \left(\frac{\mu_t}{\sigma_t} \frac{\partial h}{\partial x_j} \right) + S_h, \quad (10)$$

- conservation equations for oxygen concentration Y_{ox} and fuel concentration Y_f

$$\frac{\partial \rho Y_i}{\partial \tau} + \frac{\partial \rho u_j Y_i}{\partial x_j} = \frac{\partial}{\partial x_j} \left(\frac{\mu_t}{Sc_i} \frac{\partial Y_i}{\partial x_j} \right) + S_{Y_i}. \quad (11)$$

The combustion was modelled with Eddy Break-Up model [15]:

$$S_{\rho} = -C_{\rho} \frac{\epsilon}{k} \min \left\{ Y_f, \frac{Y_{ox}}{s} \right\}. \quad (12)$$

Radiation was taken into consideration as a heat sink term (the energy fraction, lost due to radiation, was $\chi = 0.3$).

The kerosene pool fire was modelled as the only fire source during the numerical calculation. Fuel inflow was modelled as a source term in the fuel concentration equation and it was situated under the lower car. The kerosene was modelled as $C_{13}H_{28}$, the heat of combustion was taken as $H_c = 41.87$ MJ/kg. The fuel consumption rate was evaluated here as

$$\text{before } \tau = 320 \text{ s } \dot{M}_f = 9.93 \cdot 10^{-7} \tau, \quad \text{after } \tau = 320 \text{ s } \dot{M}_f = 12.42 \cdot 10^{-6} (\tau - 294.4).$$

The natural convection type of flow existed inside of garage during the period of fire before the suppressant injection, $\tau = 0..520$ s. The calculation domain with free boundaries was used for modelling at this stage. Then, in the period $\tau = 520..624$ s, when a big amount of suppressant was injected into the compartment, the flow type changed to the forced convection. The smaller calculation domain without free boundaries and boundary conditions with equal inflow and outflow mass rates were used.

The time step was taken as follows: for the fire modelling $\Delta\tau = 1$ s, during the suppressant injection - $\Delta\tau = 0.2$ s during the period $\tau = 520..530$ s and $\Delta\tau = 0.5$ s during $\tau = 531..624$ s.

Initial and Boundary Conditions

The boundary conditions for the calculation domain with free boundaries were:

- at inflow part of free boundary, the enthalpy and species concentrations were equal to the ambient, $h = h_{amb}, Y_i = Y_{i,amb}$;
- at outflow part of free boundary, the outflow boundary conditions were used, $\partial h / \partial n = 0$, $\partial Y_i / \partial n = 0$;

all walls and internal structures were considered as adiabatic and impermeable obstacles, $\partial h/\partial n = 0$, $\partial Y_i/\partial n = 0$.

For calculation domain without free boundaries, the outflow boundary condition $\partial\Phi/\partial n = 0$ was used for all scalar variables at the outlet (check-valve). All other boundary conditions were the same as they were described above.

At initial moment, velocities, enthalpy, suppressant and fuel concentration were equal to zero and the garage was filled with air: $u_i = 0$, $h = h_{amb}$, $Y_{spr} = 0$, $Y_{fl} = 0$, $Y_{ox} = 0.23$. The initial temperature was equal $T = 293$ K.

Extinguishing Model

The simple and reliable extinguishing model, which was used for the modelling of the aerosol fire extinguishing [6], was applied in this research. The model uses the flame extinguishing concentration of suppressant Y_{spr}^* as a criterion of fire suppression: the flame is extinguished when the concentration of suppressant Y_{spr} in considered control volume is higher than the flame extinguishing concentration Y_{spr}^* and, then, the fuel consumption rate S_{fl} in this control volume is set to zero. This model doesn't need extra computer power, its precision is high enough for engineering problems and flame extinguishing concentrations are well known for a big number of industrial suppressants, used in practice. The volume concentration of the suppressant $v_{spr}^* = 0.31$ was used as a flame extinguishing concentration [16].

RESULTS OF EXTINGUISHING MODELLING

The HRR behaviour for all three methods of suppressant injection (radial spreading, one nozzle flow, three nozzle flow) is shown on Figure 5. Generally, behaviour of HRR doesn't reflect the effectiveness of extinguishing system as it depends on fire source position. We can note that the fire extinguishing was achieved for all injection cases, but it was achieved in a different time and in a very different manner.

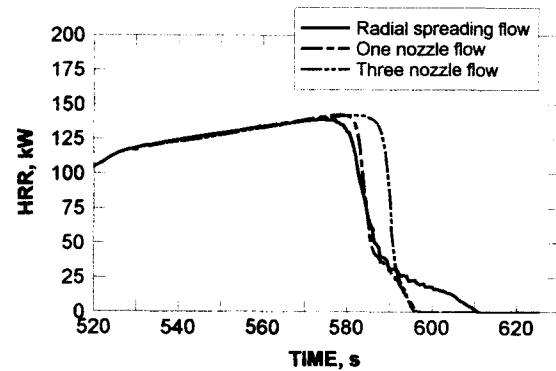


FIGURE 5. Heat release rate for different injection methods during the fire suppression

The extinguishing begins in the earliest time for the radial spreading flow, $\tau = 575$ s, but it goes relatively slow, with fluctuations at some intermediate period. Otherwise, the extinguishing for one nozzle and three nozzle cases shows very quick, almost abrupt decrease of HRR with the earlier time of fire suppression, $\tau = 595$ s. It needs to say that in this case the distance between the fire source and the nozzle location is bigger than for the radial spreading. It is the certain sign of the more uniform and effective suppressant mixing for one nozzle and three nozzle flows.

The mass of suppressant, which is left in the compartment after the suppressant was discharged completely, is presented in Table 2 in comparison with results for isothermal mixing. We can see that the mass of suppressant is almost the same for all three injection methods. Also it is easy to see that the results of calculation during the fire extinguishing and for isothermal mixing don't differ too much from each other. This is caused by a low HRR, used in the experiment and adopted in present simulation, and, consequently, low temperatures in compartment.

TABLE 2. Mass of suppressant, left in compartment, for different numerical solutions (with equal inflow-outflow mass rates boundary conditions), kg

	Simulation under isothermal conditions	Simulation of fire suppression
Radial spreading flow	96.4	95.4
One nozzle flow	97.2	97.1
Three nozzle flow	98.2	94.9

Finally, we can conclude that the analytical solution for the perfect isothermal mixing can provide us the reliable value of the suppressant mass in compartment. From the other side, this suppressant mass can not represent the effectiveness of suppressant mixing process and a reliability of extinguishing system in total, as it is a rather conservative and mean characteristic of the complex, three dimensional process. The modelling and the comparison of fire suppression results for different injection methods and fire source positions can deliver the more useful information. For extinguishing system design, the details of non-uniform suppressant distribution must be taken into account, which is possible with the use of relatively cheap, at the moment, CFD technique.

CONCLUSION

This paper presents the results of theoretical and numerical investigation of a gaseous suppressant injection and the CFD modelling of the fire extinguishing for conditions of the real fire extinguishing experiment.

The comparison of results for different boundary conditions and temperatures in compartment showed that the constant mass rate at inflow and at outflow can be used for the modelling of a suppressant propagation at initial stage of fire under considered experimental conditions.

The CFD simulation of fire and its further gaseous extinguishing were performed. The simplified, cost-effective problem formulation with a low grid number of calculation domain was used for the modelling of the gaseous fire extinguishing.

Three different suppressant injection methods were studied numerically. The one-nozzle, high-speed suppressant flow showed the most effective mixing of suppressant and the most effective extinguishing.

It was demonstrated that such an integral characteristic as a mass of suppressant in compartment is relatively insensitive to the suppressant distribution and it can not represent the effectiveness of a gaseous extinguishing system.

REFERENCES

1. Novozhilov, V., Moghterady, B., Fletcher, D.F., Kent, J.H., "Numerical Simulation of Enclosed Gas Fire Extinguishment by a Water Spray", *J. Applied Fire Science*, 5:2, 135-146, 1995/1996.
2. Novozhilov, V., Moghtaderi, B., Kent, J.H., Fletcher D.F., "Solid Fire Extinguishment by Water Spray", *Fire Safety Journal*, 32, 119-135, 1999.
3. Prasad, K., Li, C., Kaisanath, K., "Optimising Water-Mist Injection Characteristics for Suppression of Coflow Diffusion Flames" in *Twenty-Seventh Symp. (Int.) on Combustion*, pp.2847-2855, The Combustion Institute, Pittsburgh, PA, 1998.
4. Lentati, A.M., Chelliah, H.K., "Dynamics of Water Droplets in a Counterflow Field and their Effect on Flame Extinction", *Combustion and Flame*, 115, 158-179, 1998.
5. Chow, W.K., Fong, N.K., "Application of the Field Modelling Technique to Simulate Interaction of Sprinkler and Fire-Induced Smoke Layer", *Comb.Sci.Tech.*, 89, 101-151, 1993.
6. Ryzhov, A.M., "Modeling of Fires and Fire Extinction in Compartments" in *First Int. Seminar on Fire and Explosion Hazards of Substances and Venting of Deflagrations*, ed. V.V. Molokov, pp. 169-280, Moscow, 1995.
7. Makhviladze, G.M., Roberts, J.R., Yakush, S.E., Agafonov V.V., "Two-Phase Flows upon Extinguishment of Compartment Fire by an Aerosol" in *Second Int. Seminar on Fire and Explosion Hazards of Substances and Venting of Deflagrations*, ed. V.V. Molokov, pp. 497-511, Moscow, 1997.
8. United Nations Environmental Programme (UNEP), *Montreal Protocol on Substances that Deplete the Ozone Layer. Report of the Halon Fire Extinguishing Technical Options Committee*, 1994.
9. *The SFPA Handbook of Fire Protection Engineering*, publ.NFPA, 1988.
10. NFPA, "Halon 1211 Systems", 12B, publ.NFPA, 1983.
11. Patankar, S., "Numerical Heat Transfer and Fluid Flow", Hemisphere, 1980.
12. Launder, B.E., Spalding, D.B., "The Numerical Computation of Turbulent Flow", *Comp. Meth. Appl. Mech. Eng.*, 3, 269-289, 1974.
13. Hossain, M.S., Rodi, W. A., "Turbulence Model for Buoyant Flows and Its Application for Vertical Buoyant Jets" in *Turbulent Buoyant Jets and Plumes*, ed. W. Rodi, Iss.6, pp.121-172, HMT Series: Oxford, England, 1982.
14. Markatos, N.C., Malin, M.R., Cox, G., "Mathematical Modelling of Buoyancy-Induced Smoke Flow in Enclosures", *Int.J. Heat Mass Transfer*, 63-75, 89:2, 1982.
15. Magnussen, B.F., Hjertager, B.H., "On Mathematical Modelling of Turbulent Combustion with Special Emphasis on Soot Formation and Combustion" in *Sixteenth Symp. (Int.) Combust.*, pp.719-729, The Combustion Institute, Pittsburgh, PA., 1976.
16. Saito, N., Ogawa, Y., Saso, Y., Liao, C., Sakei, R., "Flame Extinguishing Concentrations of N₂, Ar, CO₂ and their Mixtures for Hydrocarbon Fuels", *Fire Safety Journal*, 27, 185-200, 1996.

MATERIALS